UNIZIK JOURNAL OF ENGINEERING AND APPLIED SCIENCES (UJEAS)

Research Article

Production of Zinc Chloride Modified Avocado Pear Seed Activated Carbon: Optimization of Preparation Conditions using ANN Modeling and RSM-Aided Box Behnken Design

Karinate Valentine Okiy, Joseph Tagbo Nwabanne, and Okwudili Obiakor

Special Issue
A Themed Issue in Honour of Professor Onukwuli Okechukwu Dominic (FAS).

This special issue is dedicated to Professor Onukwuli Okechukwu Dominic (FAS), marking his retirement and celebrating a remarkable career. His legacy of exemplary scholarship, mentorship, and commitment to advancing knowledge is commemorated in this collection of works.

Edited by
Chinonso Hubert Achebe PhD.
Christian Emeka Okafor PhD.

UJEAS

UNIZIK JOURNAL OF ENGINEERING AND APPLIED SCIENCES

UNIZIK Journal of Engineering and Applied Sciences 4(1), March (2025), 1719 - 1739
Journal homepage: https://journals.unizik.edu.ng/index.php/ujeas
PRINT ISSN: 2992-4383 || ONLINE ISSN: 2992-4391

Production of Zinc Chloride Modified Avocado Pear Seed Activated Carbon: Optimization of Preparation Conditions using ANN Modeling and RSM-Aided Box Behnken Design

Karinate Valentine Okiy[1*], Joseph Tagbo Nwabanne[1], and Okwudili Obiakor[2]

[1]Department of Chemical Engineering, Faculty of Engineering, Nnamdi Azikiwe, Nigeria.
[2]Department of Chemical Engineering, College of Engineering, Michigan Technological University, Houghton, Michigan, USA.
*Corresponding Author's E-mail: karinateokiy@gmail.com

Abstract
The exploration of the Zinc chloride activated avocado pear seed (ZAPS) production process employing Response surface methodology aided Box Benhken design and Artificial neural network algorithms was the main focus of this research. During the study, ANN and RSM models were deployed to assess the effect of process settings such as impregnation ratio, activation time and temperature on the measured BET surface of ZAPS. The RSM and ANN BET neural models were comparatively analyzed to ascertain the optimal process settings to produce the best response (BET surface area). The Analysis of Variance (ANOVA) outcome unveiled that the key independent variable(s) were activation temperature and impregnation ratio for $ZnCl_2$ modified avocado pear seed (APS) fabrication. The optimum preparation conditions for developing maximal BET surface area of 457.16 $m^2.g^{-1}$ were impregnation ratio (0.84), activation time (67.64) and activation temperature (813.94°C). The ANN neural model was ascertained to be the better model with respective root-mean-square-error (RMSE) and overall regression coefficient (R) of 31.93 and 0.9838. Sensitivity analysis outcome revealed that temperature of activation had the predominant effect on ANN model performance with sensitivity (S) value of 88.9%. This study demonstrated that ANN neural network and RSM can be applied as effective tools for optimization of the avocado pear seed (APS) alkali activation process.

Keywords: Statistical Modeling; Alkali Activation; Avocado Pear Seed Biomass Derived Adsorbents; Machine Learning Algorithms; Sensitivity Analysis.

1. Introduction

Wastewater is used water originating from municipal and industrial sources in addition to groundwater infiltration and storm water (Howard et al. 1986). Wastewater is subdivided into two major classes dependent on the nature of the activity generating the wastewater: municipal and industrial wastewater. Municipal wastewater mainly emanates from residential and commercial activities (i.e. cooking, cleaning, sewage disposal) in urban areas. Whilst, industrial wastewater emanates from different industrial processes utilizing organic and inorganic chemicals. Characteristics of inorganic and organic industrial wastewaters include dissolved organic compounds, biodegradable organics, oils, heavy metals, mineral oils, fats, acids, cyanide, dyes, detergents e.t.c (Palani et al., 2021; Kato and Kansha., 2024). These toxic impurities present in the untreated industrial effluents normally discharged into surface water bodies (i.e streams, lakes, rivers), ultimately find their way into the fresh water supply (underground aquifer) and have malignant effects on human health and environs (Bodzek et al. 2020; Ibrahim et al. 2021). Different wastewater treatment technologies exist for remediation of contaminated industrial effluents including membrane separation, electro-winning, electroflotation, chemical flotation, reverse osmosis, membrane filtration and adsorption (Srivastava et al., 2015).

Adsorption separation is the preferable technology due to technical simplicity, ease of operation, cost-effectiveness and possibility of adsorbent regeneration (economic potential) (Ali et al. 2016). Commercially produced activated carbons are expensive and non-renewable, thus unsustainable for adsorption treatment applications. Consequently, agricultural wastes (i.e. avocado pear seed) derived activated carbons are emerging as porous materials of interest (Ighalo et al. 2022). Notably, avocado pear seed are utilized in huge quantities by the general populace, mainly for culinary applications. The avocado pear seed by-products are normally discarded as wastes contributing significantly to waste disposal problems. Thus, improper disposal of waste avocado pear seeds constitutes a serious solid waste management problem. The valorisation of avocado pear seed wastes into valued-added products such as activated carbons can promote sustainable waste management and reduce environmental pollution. This is because avocado pear seed bio-resources are low-cost, abundant, inexhaustible and environmentally benign (Ighalo et al. 2022).

The adsorptive characteristics of activated carbons encompassing, rate of adsorption (mass transfer), overall effectiveness and adsorptive capacity are indicated by the BET surface area. It follows that, the performances of activated carbons are characterized industrially using BET surface area (Dyk., 2000). The physical properties of active carbons are contingent on the precursor material and preparation conditions (i.e. impregnation ratio, activation temperature, and holding time). Impregnation ratio defined as the weight of activating agent mixed with source material, has a major effect on the physical properties of the active carbons. A number of research workers have successfully produced avocado pear seed (APS) activated carbons utilizing common activating reagents such as NaOH and K_2CO_3 (Zhu et al., 2016; Haki et al. 2021). A conspicuous omission is that the preparation of APS derived activated carbons using $ZnCl_2$ activating agent has seldom been performed, which necessitates intensive research emphasis. Furthermore, optimization of preparation conditions to minimize production times and enhance BET surface area is important, but seldom performed for $ZnCl_2$ modified APS. Modern process modeling and optimization often employ techniques such as Response Surface Methodology (RSM), Artificial Neural Networks (ANN), and Adaptive Neuro-Fuzzy Inference System (ANFIS). These methods have been proven to be effective in modeling and simulation complex physical systems (Chebii et al., 2022; Du et al., 2024).

Hence, the novelty of this study is centred on the synergistic use of data-driven techniques (i.e. RSM and ANN) to optimize the preparation conditions of $ZnCl_2$-modified APS, thereby providing a holistic understanding of the factors governing its adsorption characteristics. This study integrates statistical (RSM) and machine learning (ANN) methods to improve the prediction accuracy of BET surface area, which directly influences adsorption efficiency. While RSM offers insights into factor interactions and optimal conditions, ANN complements it by capturing non-linear relationships within the dataset, thus overcoming the limitations of conventional statistical methods (Chebii et al. 2022). The successful application of ANN and RSM in this study marks a significant advancement in the field of activated carbon optimization, setting a new precedent for future investigations into biomass-derived adsorbents.

Accordingly, this research proposes to (i) investigate the production of active carbons from avocado pear seeds with basic activation ($ZnCl_2$) (ii) utilize RSM-BBD model for selection of optimum $ZnCl_2$ modified APS with maximal BET surface area (iii) develop an ANN model for optimizing the production of APS derived carbon under different process conditions of activation time, temperature and base/precursor mixing ratio (iv) analyse the carbon fabrication process using both ANN and RSM-BBD models to ascertain their prognostic performances for the $ZnCl_2$/APS system (v) assess the impact of independent variable(s) on neural network predictions using sensitivity analysis.

The innovative aspect of this study lies in its fusion of experimental optimization with advanced computational intelligence to enhance process efficiency and adsorption performance(s). By harnessing learning machine techniques alongside conventional optimization strategies, this study provides a transformative approach to sustainable wastewater treatment solutions, advancing both environmental engineering and material science frontiers.

2.0 Materials and methods

2.1 Active Carbon production

The raw avocado pear seeds were sourced from Eke-Awka Market in Awka South Local Government Area, Anambra State, Nigeria (N: 6° 13’ 8”; E: 7° 5’ 13”). The chemical activation of these seeds with zinc chloride was carried out following the methodology outlined by Zhu *et al.* (2016) (refer to Figure 1). Initially, 300 grams of fresh avocado pear seeds were cleaned by washing with 5000 grams of deionized water and 3945 grams of ethanol to eliminate surface impurities. The cleaned seeds were subsequently dried in a Mermmert air-circulating oven at 383 K for 24 hours. Once dried, the seeds were cut into smaller pieces, ground using a Jencod grinding machine, and sieved through a 300 µm Taylor sieve. For the activation process, 100 grams of dried avocado pear seed powder was soaked in a 36.5 gram solution of 30% zinc chloride at different impregnation ratios (0.5:1, 1:1, and 1.5:1) for 2 hours. This was followed by drying in a Mermmert oven at 368 K for 24 hours. The dried $ZnCl_2$- treated samples were then subjected to thermal activation in a muffle furnace at varying temperatures (873 K, 1023 K, and 1173 K) and durations (60, 90, and 120 minutes). During activation, a consistent heating rate was maintained until the target temperatures (873 K, 1023 K, and 1173 K) were reached, after which the samples were held at these temperatures for the designated durations.

After activation, the samples were cooled to room temperature and thoroughly washed with distilled water until the solution pH stabilized at 7.0, ensuring complete removal of residual $ZnCl_2$. The samples were further treated by immersing them in a 250 ml solution of 0.1 M HCl for 1 hour, followed by repeated washing with distilled water until a pH range of 6–7 was achieved. The resulting activated carbon samples were then filtered using Whatman No.1 filter paper and dried in a Mermmert oven at 348 K for 24 hours. The BET surface area of the activated carbons was determined based on nitrogen adsorption at varying pressures using the Brunauer-Emmett-Teller (BET) method, conducted via a Quantachrome NOVA4200e BET Analyzer (Anton Paar GmbH, Austria).

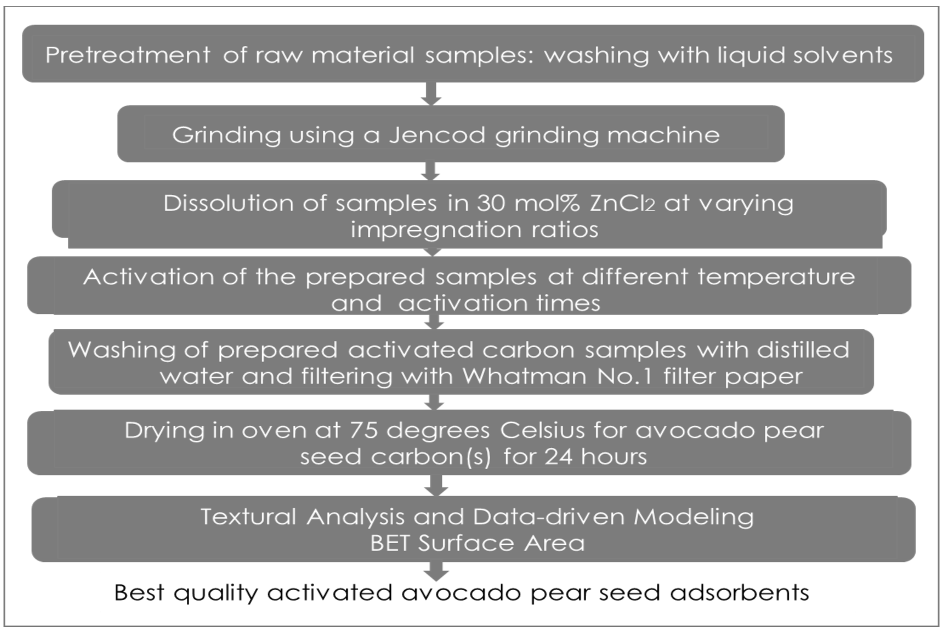

Figure 1: Diagrammatic illustration of the zinc chloride modified avocado pear seeds production process.

.

2.2 Experimental design by Box Behnken (BBD)

Response Surface Methodology was utilized as the statistical modelling technique to (i) assess the effects of single factors on the response of interest (ii) determine the two-factor interaction effects of the independent variables and (iii) optimise the achievable BET surface area of zinc chloride activated avocado pear seed carbon (Anderson and Whitcomb, 2016). The RSM optimisation scheme for the APS activated carbon synthesis was evaluated with the aid of BBD. In this study, the variables chosen for analysis were activation temperature, activation time, and impregnation ratio. The response variable selected was the BET Surface area (m^2/g). The upper and lower bounds of the independent variables for the BBD are presented in Table 1. The experimental ranges were determined based on previous literature, specifically Buasri *et al*. (2023). The total number of experimental runs for the BBD design was calculated using Equation 1.

$$N = K^2 + K + +C_P \quad [1]$$

Where, N represents the total number of treatment combinations, C_P denotes the number of replicates at the centre point and K corresponds to the number of factors (Melvin *et al.* 2015).

A three-level, three-factor Box-Behnken Design (BBD) was utilized, consisting of 48 treatment combinations, including 2^2 factorial points arranged in an incomplete block design (IBD) along with six center points leading to a total of 54 experimental runs, as shown in Table 2. The factorial points ensured a well-distributed range of high and low values, while the central points contributed to maintaining data reliability and provided an estimate of experimental error (Onu *et al.* 2021). The statistical analysis was carried out using Minitab 19.1 (Minitab LLC, USA) to model and predict the response of the $ZnCl_2$/APS system. To minimize systematic errors, all 54 experimental runs were conducted in a disorderly manner ensuring variability in the independent variables, whilst following the design of experiments (DOE) matrix.

Table 1: Variables and their corresponding levels for the BBD design.

Independent Variable(s)	Range and Level		
	-1	0	+1
Activation temperature (A, ^{0}C)	600	750	900
Activation time (B, mins)	60	90	120
Impregnation ratio (C)	0.5	1.0	1.5

The Box Behnken design (BBD) was arranged using a spherical pattern, where each factor was assigned coded values of 1, 0 and -1 to signify high, medium and low levels, respectively, while maintaining equal spacing between them (Anderson and Whitcomb, 2016) as shown in Table 1.

Table 2: Box-Behnken Experimental Design Matrix for Zinc Chloride Activation of Avocado Pear Seeds.

Run order	Activation Temp (^{0}C)	Activation Time (Mins)	Impregnation ratio Activating agent: raw material	BET Surface Area (m^2/g)
1	600	60	1.0	555.4
2	900	60	1.0	530.3
3	600	120	1.0	636.5
4	900	120	1.0	574.5
5	600	90	0.5	294.5
6	900	90	0.5	791.5
7	600	90	1.5	879.4
8	900	90	1.5	889.9
9	750	60	0.5	903.1
10	750	120	0.5	774.7
11	750	60	1.5	836.0
12	750	120	1.5	921.0
13	750	90	0.5	695.6
14	750	90	0.5	695.6
15	750	90	0.5	695.6
16	600	60	1.0	555.4
17	900	60	1.0	530.3
18	600	120	1.0	636.5
19	900	120	1.0	574.5
20	600	90	0.5	294.5
21	900	90	0.5	791.5
22	600	90	1.5	879.4
23	900	90	1.5	889.9
24	750	60	0.5	903.1
25	750	120	0.5	774.7

26	750	60	1.5	836.0
27	750	120	1.5	921.0
28	600	60	1.0	555.4
29	900	60	1.0	530.3
30	600	120	1.0	636.5
31	900	120	1.0	574.5
32	600	90	0.5	294.5
33	900	90	0.5	791.5
34	600	90	1.5	879.4
35	900	90	1.5	889.9
36	750	60	0.5	903.1
37	750	120	0.5	774.7
38	750	60	1.5	836.0
39	750	120	1.5	921.0
40	600	60	1.0	555.4
41	900	60	1.0	530.3
42	600	120	1.0	636.5
43	900	120	1.0	574.5
44	600	90	0.5	294.5
45	900	90	0.5	791.5
46	600	90	1.5	879.4
47	900	90	1.5	889.9
48	750	60	0.5	903.1
49	750	120	0.5	774.7
50	750	60	1.5	836.0
51	750	120	1.5	921.0
52	750	90	0.5	695.6
53	750	90	0.5	695.6
54	750	90	0.5	695.6

Moreover, the reduction empirical model for the $ZnCl_2$-APS fabrication process can be expressed using the following second-order approximating polynomial equation based on coded factors (Okiy and Nwabanne., 2024):

$$Y = b_0 + \sum_{i=1}^{n} b_i X_i + \sum_{i=1}^{n} b_{ii} X_i^2 + \sum_{i=1}^{n-1}\sum_{i=2}^{n} b_{i,j} X_i X_j + E \qquad [2]$$

Where, b_0, b_i, b_{ij} and b_{ii} are the constant coefficients of the intercept, linear, and interaction terms respectively, n is the number of patterns, Y is the calculated dependent variable, i and j are index numbers, the term E accounts for errors, whereas X_i, and X_j signify the independent factors under investigation.

2.3 Artificial Neural Network modeling

The artificial neural network (ANN) is a non-linear numerical mapping between the numeric inputs and output dataset(s) for detection of a suitable generalization of the actual system (Basu., 2013). The ANN training process involves the following steps: (i) reset of network weights (ii) summation of input data and bias, before transfer of result through the activation function to obtain the output signal(s) (iii) comparison of network model prediction with the labelled data to determine performance function (MSE) value (iv) reiterative adaptation of network parameters (weights) using the back-propagation training algorithm to minimize performance function (MSE) error and satisfy the convergence criteria.

The MLP feed-forward neural network model was constructed using MATLAB R2019b version 9.9 (MathWorks Inc, USA) to predict the achievable BET surface area of $ZnCl_2$-activated APS. The Multi-Layer Perceptron feed-forward neural network with back-propagation training algorithm was utilized in deciphering the complicated associations between the independent variables, input parameters (i.e number of hidden layers, number of neurons) and measured (labelled) data (Chebii *et al*. 2022). Factors such as alkali impregnation ratio, activation time and temperature, were selected as input (independent) variables to the neural network model. In addition, the response variable-BET surface area was chosen to be the dependent factor. The multi-layer perceptron network is well-regarded for its ability to model noisy and non-linear data (Chebii *et al.* 2022).

The ANN network proposed in this study features dual hidden layers, an input and one output layer (Figure 2). A two hidden layer ANN model was selected for this research, due to its enhanced predictive performance compared to a single hidden layer (Jerry, 2002). The ANN was designed with a sigmoid mathematical function for the neurons in both hidden layer(s), whilst the input and output layers were modeled utilizing a linear mathematical function.

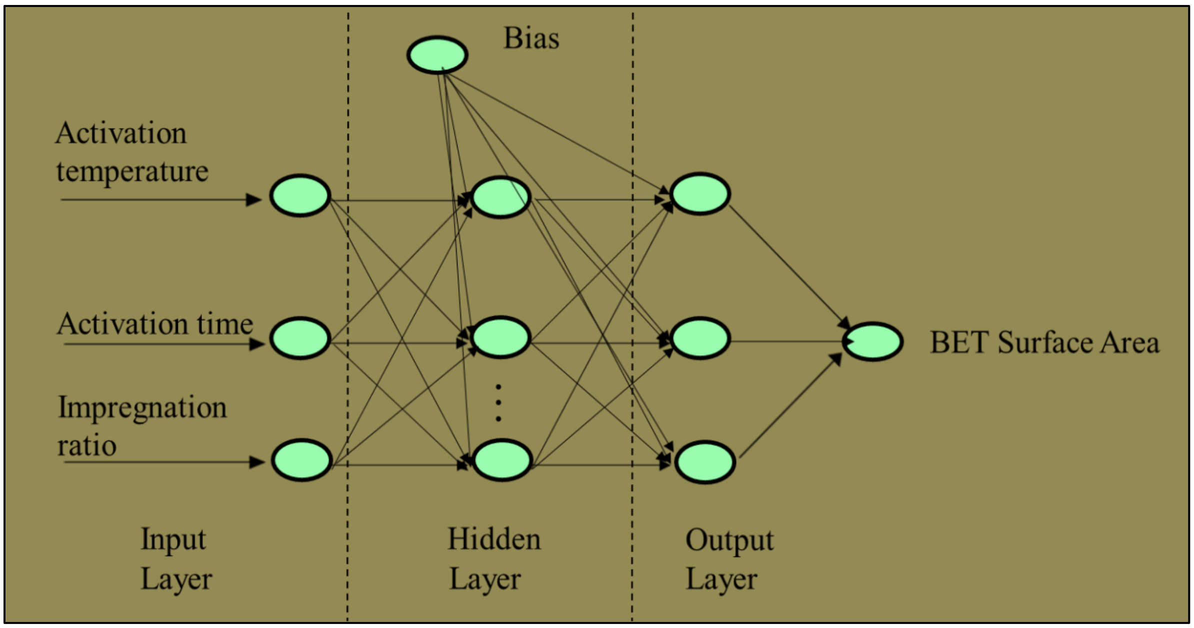

Figure 2: Artificial Neural Network topology for modeling the $ZnCl_2$/APS system.

To forestall over-fitting, the number of hidden layer neurons were determined based on the hush heuristic method, suggesting that the optimal number of neurons is 3 times the number of independent (input) variables (Alkhasawneh., 2021). Consequently, nine neurons were specified to be imbedded in the hidden layer(s) of the ANN model. According to Onu *et al.* 2021, network modeling of a non-linear system with larger dataset is better than using a smaller number of data points. Consequently, the experimental dataset for alkali avocado pear seed activation was increased four-fold, providing a total of 54 datum utilised for the ANN network modeling, of which 70% (38 records) were used for training, 15% (8 records) were used for validation, and the remainder records for testing. The ANN network (3:5:4:1) incorporating the three abovementioned input variables, nine hidden neurons, and one output variable was found to be appropriate for calculating the achievable BET surface area(s) of $ZnCl_2$-activated avocado pear seed (Figure 3).

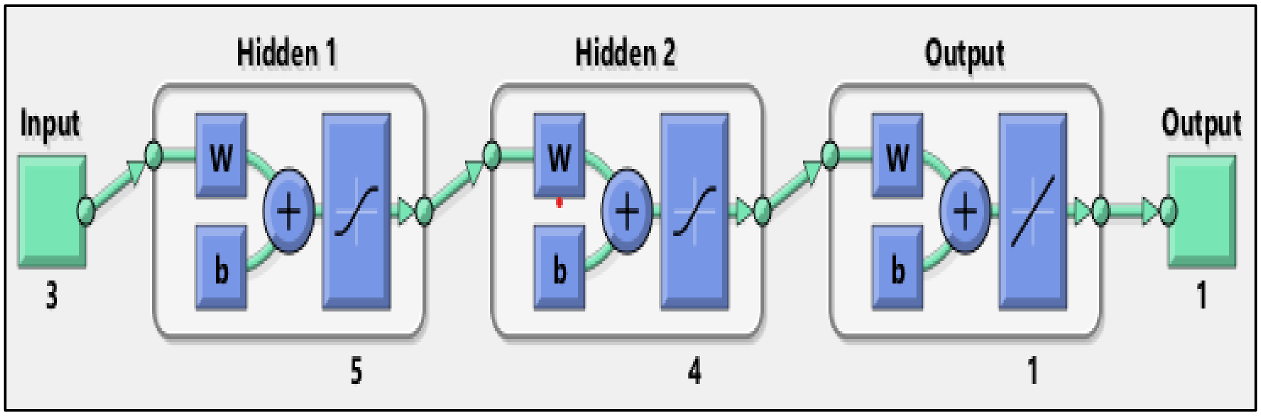

Figure 3: Configuration of ANN BET network with nine hidden-layer neurons.

The ANN model training was performed utilizing a neural network code that automatizes the neural network training process.

3.0 Result and Discussion

3.1 Modeling of the ZAPS activation process using RSM-BBD

A total of 54 individual experiments were carried out to produce APS derived activated carbons according to Box Behnken experimental design matrix presented in Table 2 and the response (BET surface areas) evaluated. Non-linear regression modeling was applied to formulate a correlation between the APS-derived carbon manufacturing process variables and response(s) using the ordinary least squares method. The most suitable model for accurately representing the experimental data and explaining the response variation of the $ZnCl_2$/APS system was identified using the Sequential Model Sum of Squares (SMSS) test. Based on the SMSS analysis results for the achievable BET surface area of $ZnCl_2$-modified APS, as shown in Table 3, Minitab Software version 19.1 recommended the quadratic model. Though, the cubic model was aliased due to the fact that the BBD experimental design does not hold enough runs to underpin a cubic model (Onu *et al*. 2021).

Table 3: Type 1 Sequential Model Sum of Squares Analysis for $ZnCl_2$-Activated Avocado Pear Seed.

Source	Sum of Squares	df	Mean Square	F-value	P-value	
Mean	$2.748E^{+07}$	1	$2.748E^{+07}$			
Linear	65.42	1	65.42			
2FI	95038.52	3	31679.51	0.9737	0.4128	
Quadratic	$1.544E^{+05}$	3	51466.63	1.64	0.1922	Suggested
Cubic	$3.599E^{+05}$	3	$1.200E^{+05}$	4.78	0.0058	Aliased
Residual	$3.360E^{+05}$	3	$1.120E^{+05}$	6.02	0.0017	
Total	$7.439E^{+05}$	40	18596.82			

The Analysis of Variance (ANOVA) for Box Behnken experimental design was then applied for assessment of the adequacy and significance of the approximating polynomial model. The goodness of fit of the second-order polynomial model was evaluated using the Adjusted R^2, coefficient of determination R^2, Standard deviation (SD), Coefficient of Variation (C.V) and Adequate precision. Utilizing the 95% significance level, factors having p-value less than 0.05 and Fisher F-value greater than critical $F_{critical}$ are considered to be statistically significant. The final response model was derived by eliminating non-significant terms (p-value > 0.05). The ANOVA results for $ZnCl_2$-activated APS are presented in Table 4.

Table 4: ANOVA results for $ZnCl_2$-activated avocado pear seed carbon.

Source	Sum of Squares	Df	Mean Square	F-Value	P-Value
Model	1315843	9	146205	17.22	0.000
A-Act. Temp	358599	1	88368	10.41	0.002
B-Act. Time	88368	1	3354	0.40	0.533
C-Impreg. Ratio	3354	1	290703	34.25	0.000
AB	266877	1	1362	0.16	0.691
AC	673661	1	236682	27.88	0.000
BC	499998	1	45540	5.37	0.025
A^2	62016	1	22819	2.69	0.108
B^2	111646	1	17645	2.08	0.156
C^2	283583	1	111646	13.15	0.001
Residual	373473	44	8488		
Std. Dev= 92.13	**R-Sqr** = 77.89%	**R-Sqr(Adj)**= 77.37%	**Adeq Precision** = 5.2997	**C.V.%**= 22.22	

The predicted response (BET surface area) for $ZnCl_2$-activated APS synthesis is represented by the following model equation [Eqn. 4]:

$$BETArea = -1422 + 7.30\times A - 15.2\times B - 573\times C - 0.00205\times A\times B - 1.622\times A\times C + 3.56\times B\times C - 0.00343\times A^2 + 0.0753\times B^2 + 830\times C^2 \quad [4]$$

The ANOVA analysis for the production process of APS-derived activated carbon (AC), presented in Table 4, reveals a p-value for the polynomial model below 0.05 (p-value = 0.000). This indicates that the polynomial model is statistically significant at a 95% confidence level. Moreover, the substantial F-value of 17.22 implies the relevance of the quadratic model, with a 0.000% chance that the observed F-value is the result of random fluctuations, reinforcing the findings from the p-value test (He *et al*. 2023). The ANOVA results indicated that the linear factors of activation temperature (A) and impregnation ratio (C), along with the quadratic term for impregnation ratio squared (C^2), had a significant effect on the response variation, as evidenced by p-values below 0.05. In addition, the interactions between activation temperature and impregnation ratio (A*C), as well as between activation time and impregnation ratio (B*C), were found to significantly affect the BET surface area, with p-values under 0.05. In contrast, the linear effect of activation time (B), the quadratic terms of activation temperature squared (A^2) and activation time squared (B^2), and the interaction between activation temperature and activation time (A*B) did not significantly influence the response, as their p-values were greater than 0.1 (Nguyen *et al*. 2022). As well, the low F-values confirmed that the variations in the Activation time, Activation temperature product, Activation time product, and Activation temperature & Activation time interaction did not significantly affect the BET surface area (Onu *et al*. 2021). Hence, it can be concluded that impregnation ratio and activation temperature were the linear terms in the polynomial model equation that significantly influenced the $ZnCl_2$-activated APS fabrication process. In general, increase in the amount of activating agent mixed with the activated carbon (AC) precursor in the range of 0.25 to 4.0 suppresses formation of chemicals (tar) and additional by-products (acetic acid and methanol) during preparation, resulting in higher AC yield. Further, optimization of final activation temperature is also important to reduce the expense and duration of ZAPS production (Marsh and Rodríguez-Reinoso, 2006). Following, the removal of all the non-significant terms, the ensuing polynomial model is obtained:

$$BETArea = -1422 + 7.30\times A - 573\times C - 1.622\times A\times C + 3.56\times B\times C + 830\times C^2 \quad [5]$$

The synergetic and antagonistic effects on attainable BET surfaces of the $ZnCl_2$-activated APS are shown by the positive and negative terms in the response model equation.
The data presented in Table 4 showed that the response model has moderate standard deviation (92.13) and high coefficient of determination values (R^2 =77.89%), signify some variability in the response variable (BET surface area) around the mean value(s) predicted by the model. In addition to the fact that approximately 77.89% of

response (BET surface area) variation(s) can be explicated by the model, typically R^2 above 75% is considered acceptable in modeling complex physical systems (Anderson and Whitcomb, 2016). Further, the model's p-value of 0.000 (P-value < 0.05) suggests that it is statistically significant at the 95% confidence level, with a 0.5% likelihood that variations in at least one of the independent variable(s) is attributable to noise (Anderson and Whitcomb, 2016). The response model also had high adequate precision (5.2997) and moderate coefficient of variation values (22.22) respectively, indicating a strong signal-to-noise ratio and confirming the model's robustness in navigating the design space (PRESS > 4) as well as moderate variance of the predicted response(s) about the mean, satisfactory for the experimental conditions (Okpe *et al.* 2018; Onu *et al.* 2021). In addition, the fairly close accordance of the adjusted R^2 value of 77.37% and R^2 value of 77.89% ($R^2 - R^2_{adj} < 20\%$) suggests that redundant predictors are not included and the response model is not over-fitting (Anderson and Whitcomb, 2016). In all, the model provides a good fit and adequately explains the variability in the response variable (BET surface area), indicating good predictive capability. The results of the measured and RSM predicted response(s) are depicted in Table 5.

Table 5: Comparison of RSM Predicted and Measured BET Surface Area for $ZnCl_2$-Activated APS.

Point	**BET Surface Area (Predicted)**	**BET Surface Area (Actual)**	**STD Error Fit**	**Square Residual**
1	502.16	555.4	0.641	308469.2
2	625.71	530.3	-1.149	9103.068
3	541.09	636.5	1.149	9103.068
4	627.74	574.5	-0.641	1116.228
5	444.34	294.5	-1.80	22452.03
6	792.69	791.5	-0.0143	1.4161
7	878.21	879.4	0.0143	7518.624
8	740.06	889.9	1.80	22452.03
9	806.50	903.1	1.163	9331.56
10	720.28	774.7	0.655	1011.24
11	890.43	836.0	-0.655	2962.625
12	1017.60	921.0	-1.163	9331.56
13	695.60	695.6	0.00	0
14	695.60	695.6	0.00	0
15	695.60	695.6	0.00	0
				RMSE= 157.54

Figure 4 presents a comparison between the BET surface area obtained experimentally and the BET surface area predicted using the RSM model.

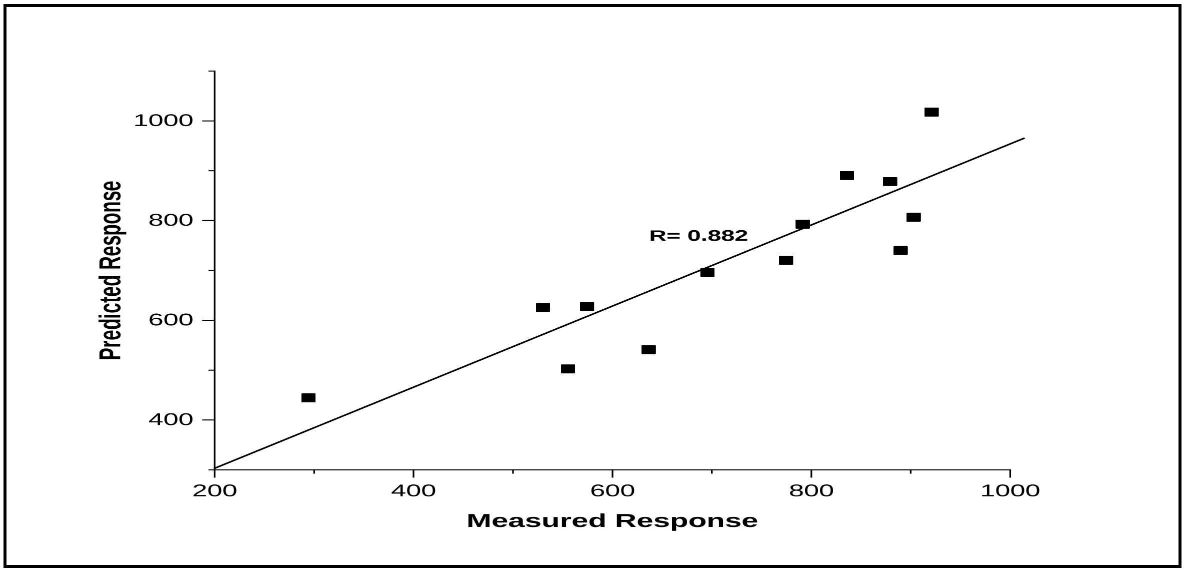

Figure 4: Cross-plot of computed BET surface area against measured data.

The cross-plot depicted in Figure 4 shows a strong agreement between computed and measured BET surface areas, with a correlation coefficient (R) value of 0.882 indicating reliable model performance (Ranade and Ranade, 2023). The R-value of 0.882 suggests that approximately 88.2% of the variance in the measured BET surface area can be explained by the computed values. This strong correlation supports the use of the model for predicting how changes in activation parameters affect BET surface area. This high correlation signifies that the model captures the underlying trends in the data effectively, though some discrepancies still exist. The deviations observed in certain data points may arise due to inability to capture the complex interactions amongst variables (inherent model limitations). Furthermore, the alignment of data points along the bisector (45^0) line indicates that the model consistently produces predictions close to the experimental values (Okiy and Nwabanne, 2024). Hence, the regression model has strong ability for predicting BET surface area(s) under similar experimental conditions, aiding in process optimization. The normal probability plot presented in Figure 5 was also utilized to evaluate the distribution of data points. The symmetry of the probability distribution on both the right and left sides of the plot indicates that the error residuals are normally distributed. This suggests that there are no apparent issues with the model or the process data (Iheanancho et al., 2019).

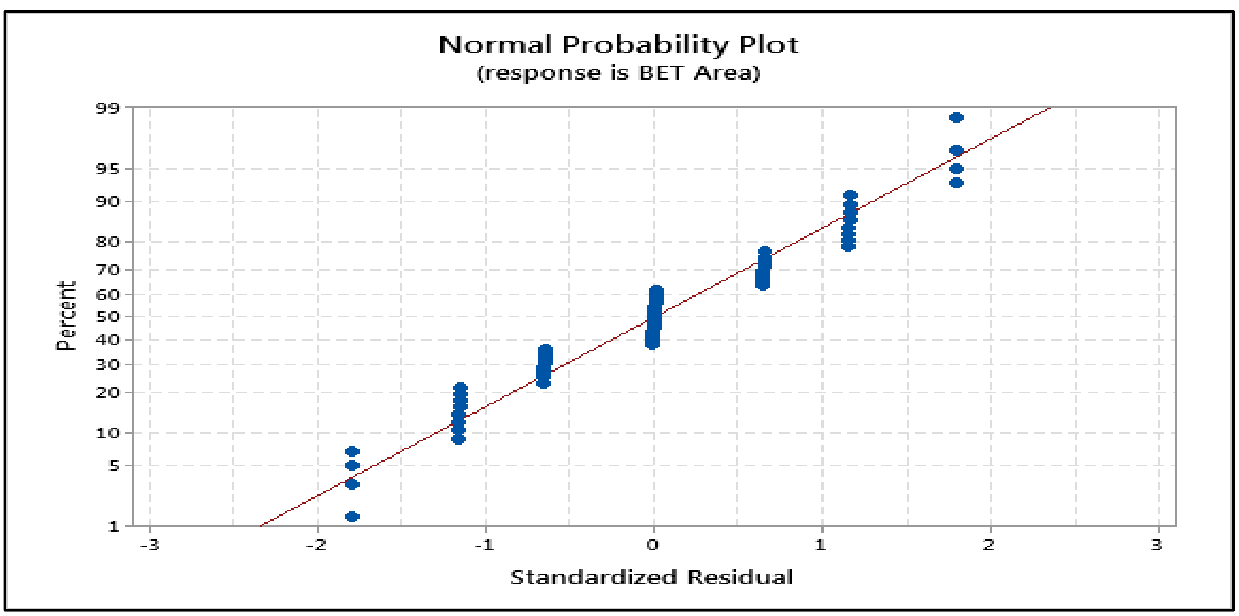

Figure 5: Normal plot of error residuals for the $ZnCl_2$/APS system.

This construal was statistically affirmed by the Shapiro-Wilk test, which produced a p-value greater 0.05 (p-value = 0.9985) and high wilk-statistic of 0.99471, confirming that the residuals follow a normal (gaussian) distribution (Figure 6).

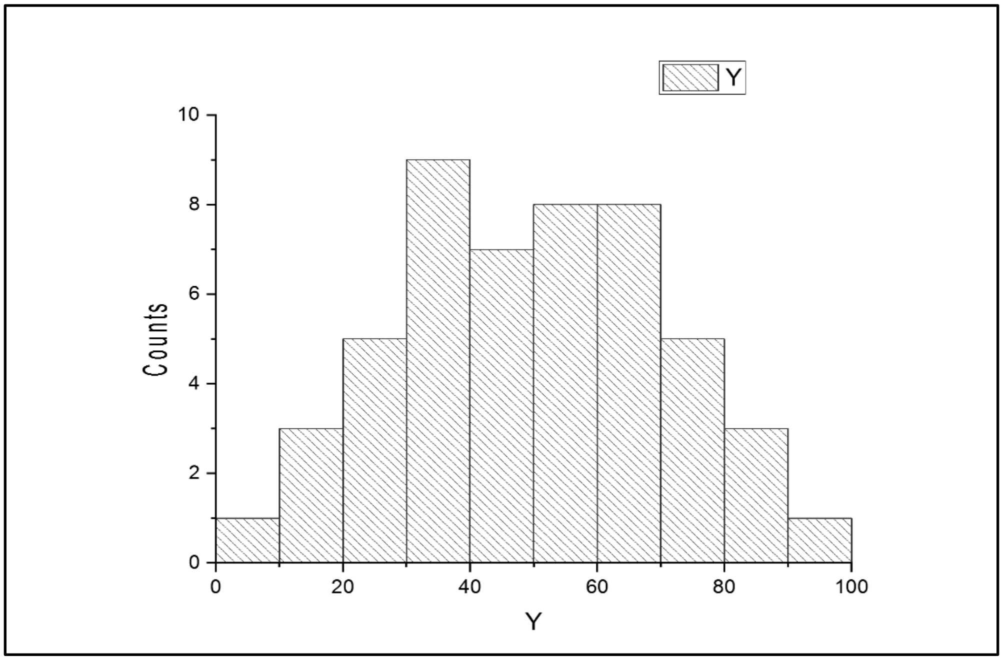

Figure 6: Histogram plot of error residuals (Y) for the $ZnCl_2$/APS system.

The importance of the estimated linear effects, interactions, and their products on the response of interest (BET surface area), in order of significance, are presented in the Pareto diagram (Figure 7). The perpendicular line shows the extent of the least statistically significant effect for a 95% confidence level, and the analogous t-test value is equal to 2.015. Any factor or its interaction that exceeds the demarcation (vertical) line is considered significant (Anderson and Whitcomb, 2016).

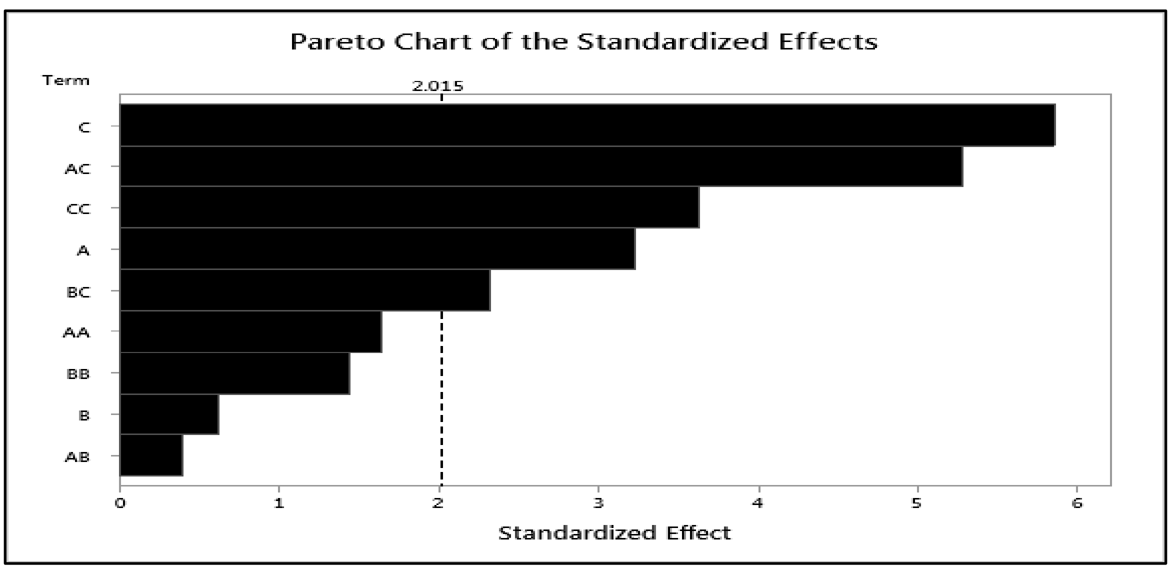

Figure 7: The Pareto plot for $ZnCl_2$-activated APS.

Figure 7 depicts that the linear effect of factor C (impregnation ratio), along with its quadratic term (C^2), are

the most significant predictor variable(s) determining the achievable BET surface area of $ZnCl_2$-activated APS.
The three-dimensional response surface plots, shown in Figures 8(a–c), were generated to visualize the relationships between the independent variables-activation temperature, activation time, and impregnation ratio and the response variable (BET surface area), considering their linear and interaction effects. These plots facilitate the optimization of the $ZnCl_2$-activated APS production process. The regression models developed for the multivariable $ZnCl_2$/APS system incorporate three independent predictors. Accordingly, each response surface diagram was plotted as a function of two factors within their respective ranges (-1 to 1), while the third factor was held constant at the central (zero) level.

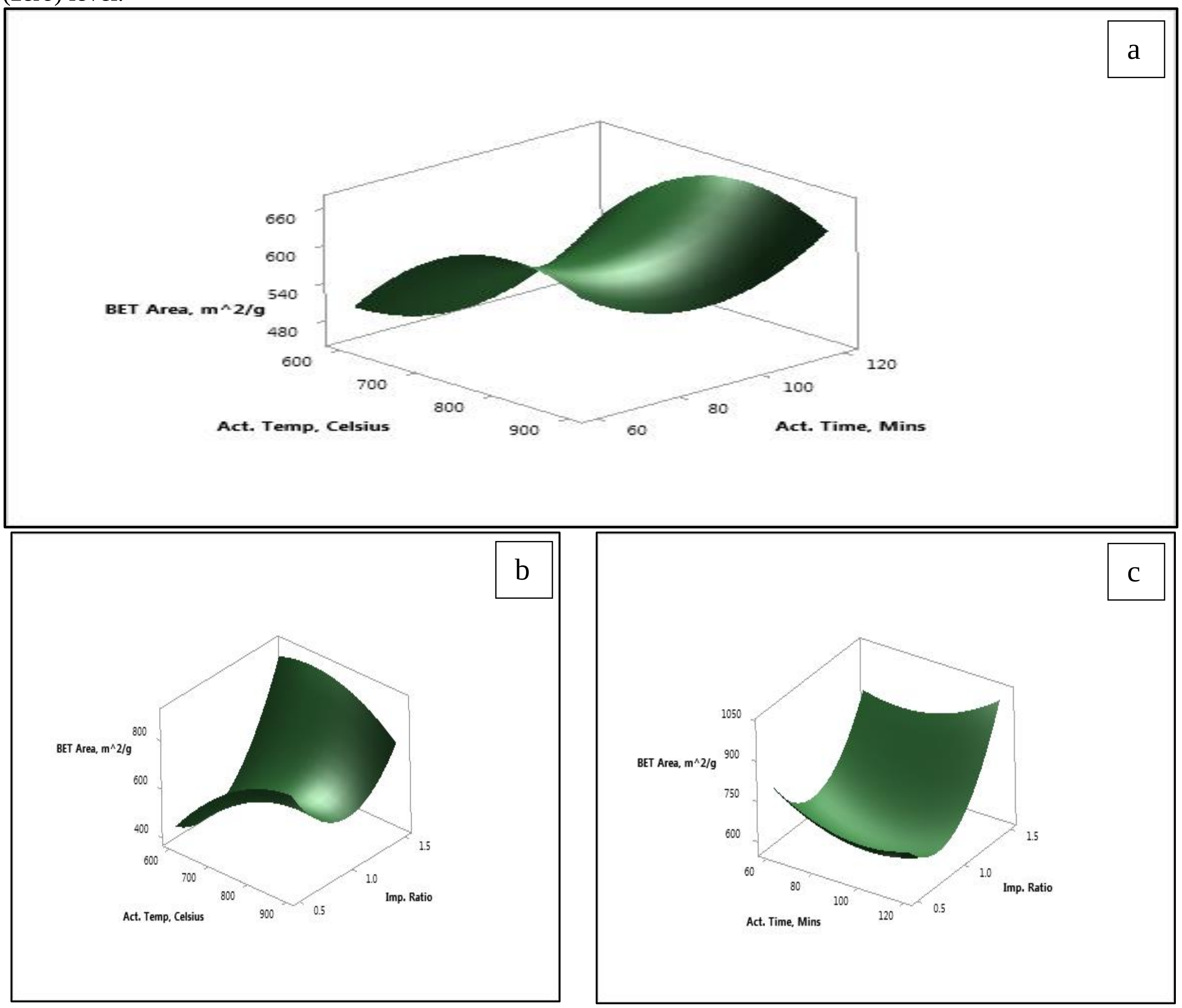

Figure 8: 3-D response surface plots illustrating the BET surface area for (a) an impregnation ratio of 1.0 (b) an activation time of 90 mins, and (c) an activation temperature of 750 ^{0}C.

Figure 8a clearly shows that the BET surface area of $ZnCl_2$-activated APS increases with rising activation temperature. Similarly, an increase in activation time also leads to a higher BET surface area, indicating a synergistic effect of both parameters on the BET surface area of $ZnCl_2$-activated APS. In Figure 8b, the BET surface area follows an increasing trend with activation temperature until it reaches a maximum. Likewise, the BET surface area rises with an increasing impregnation ratio before reaching an optimal point. As seen in Figure 8c, the BET surface area declines as activation time increases, reaching a minimum. However, it continues to increase with a higher impregnation ratio until it attains a peak point. In all instances, the impregnation ratio plays a more significant role relative to activation temperature and extent of activation (activation time) in the ZAPS activated carbon synthesis process. This connotes that impregnation ratio had a predominant effect on the achievable BET surface area of $ZnCl_2$-activated APS.

From the statistical optimization results, the best BET surface area achieved for $ZnCl_2$-activated APS was 457.163 $m^2.g^{-1}$ with an activation time of 67.6 minutes, activation temperature of 813.94^{0}C, and an impregnation ratio of 0.840. Subsequent experimental treatments using the optimum conditions yielded an observed BET surface area of 460.62 $m^2.g^{-1}$ (Table 6). These result(s) confirmed the validity of the polynomial response model developed using RSM.

Table 6: Measured and predicted value of achievable BET surface area for $ZnCl_2$-activated avocado pear seeds using optimal activation conditions.

Optimal Conditions				**BET Surface Area (m^2/g)**	
No of Replicates	Activation Time, mins	Activation Temperature, ^{0}C	Impregnation ratio	Experimental	Predicted
1	67.640	813.94	0.840	460.62	457.163

3.2. ANN modeling of the APS alkali activation process

The ANN model was implemented using MATLAB version 9.4 (R2018a). The network design of the neural model comprises of a single input layer with three independent variables, two hidden layers with nine hidden neurons, in conjunction with one output layer as aforeshown (See Figure 3). Statistical indices such as correlation coefficient (R) and Root-Mean-Square-error (RMSE) were utilized to establish the computational accuracy and performance limits of the created ANN BET model for $ZnCl_2$-activated APS synthesis (Chebii *et al.* 2022; Ranade and Ranade., 2023).

The ANN model performance plot of error function (MSE) with respect to the number of training cycles (Epochs) for the ZAPS activation process is presented in Figure 9. The best validation performance of 5.05 × 10^{-20} was achieved at 22 Epochs. The low value of the MSE determined, evinces that the model performance plot did not show any indications of over-parametization (over-fitting). In addition, the training (blue) and validation (green) curves are alike and in close proximity to the best fitting curve for this instance. Consequently, over-fitting problems are not likely to occur with the trained ANN model. Moreover, the validation curve exhibited a significantly greater increment in the latter stages of iterations through the training dataset relative to smaller increment of the test curve in the earlier epochs, indicative of little possibility of over-fitting incidents (Onu *et al*. 2021).

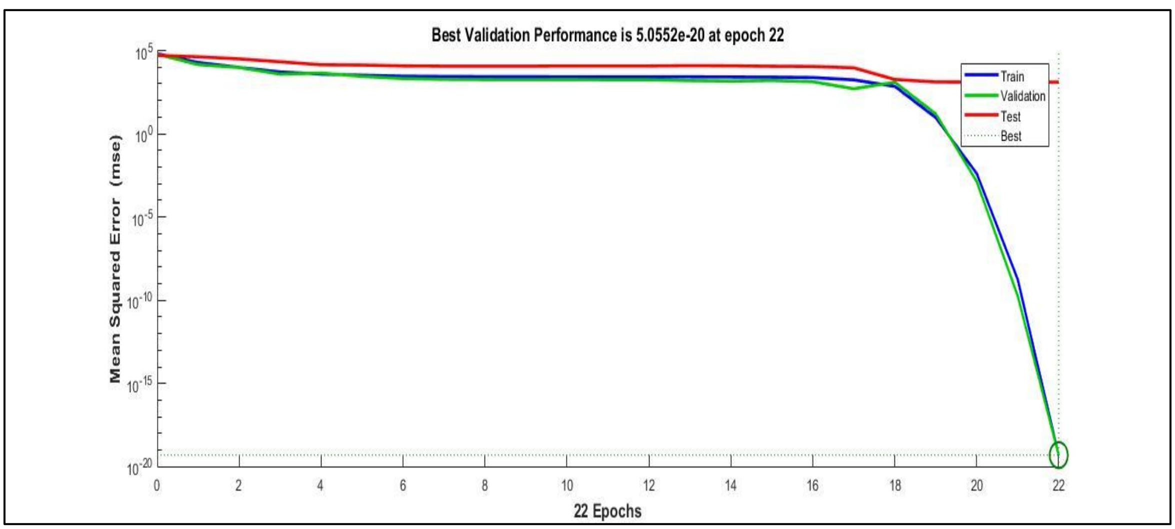

Figure 9: ANN Model Performance chart for ZAPS activation process.

Figure 10 presents the regression plots for training, testing, and validation of the neural network model. The optimal ZAPS activation model exhibited correlation coefficients (R) of 0.9979 for training, 0.98945 for testing, and 1.0 for validation, resulting in an average R-value of 0.99738. This high correlation suggests a strong relationship between the input variables and the neural network predictions for BET surface area (0.995 < Ravg = 0.99738) (Ranade and Ranade, 2023). In addition, this construal is supported by the relatively low root mean square error (RMSE) of 31.93.

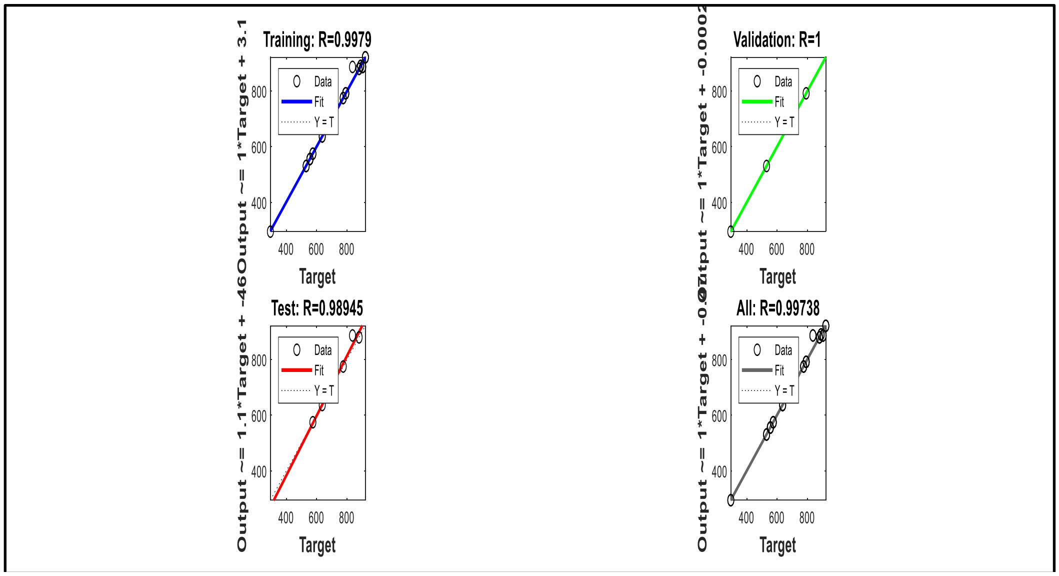

Figure 10: ANN Regression plots for training, testing, validation, and overall data.

To valuate the precision of the ANN neural model in reproducing the labelled data used in network training. The measured BET surface area(s) were compared with the ANN-predicted values at varied preparation conditions as shown in Table 7. As apparent from the low value of RMSE (See Table 7), the observed and ANN model predicted results matched reasonably well (31.93). The minimum RMSE value demonstrates that the hidden layers of the ANN effectively recognized the training patterns, leading to improved predictive accuracy (Chebii *et al*., 2022). This outcome suggests that the ANN BET model reliably replicates the experimental data for the APS alkali activation process.

Table 7: Comparison of ANN outputs with observed results for the manufacture of $ZnCl_2$- activated APS.

Point	**BET Surface Area m^2/g (ANN)**	**BET Surface Area m^2/g (Experiment)**	**Residual Square**
1	555.4	555.4	$1.0611E^{-20}$
2	530.3	530.3	$3.23E^{-22}$
3	736.29	636.5	9957.30
4	574.5	574.5	$7.821E^{-22}$
5	294.5	294.5	$2.551E^{-22}$
6	791.5	791.5	$1.047E^{-24}$
7	879.4	879.4	$6.154E^{-20}$
8	889.9	889.9	$1.324E^{-20}$
9	903.1	903.1	$4.864E^{-22}$
10	687.45	774.7	7613.179
11	836	836	$1.204E^{-19}$
12	921	921	$1.847E^{-21}$
13	695.6	695.6	$9.562E^{-22}$
14	695.6	695.6	$9.562E^{-22}$
15	695.6	695.6	$9.562E^{-22}$
			RMSE = 31.93

Further, the ANN BET model was assessed by comparing the network output(s) with the experimental results for the calculated BET surface area(s), as shown in Figure 11.

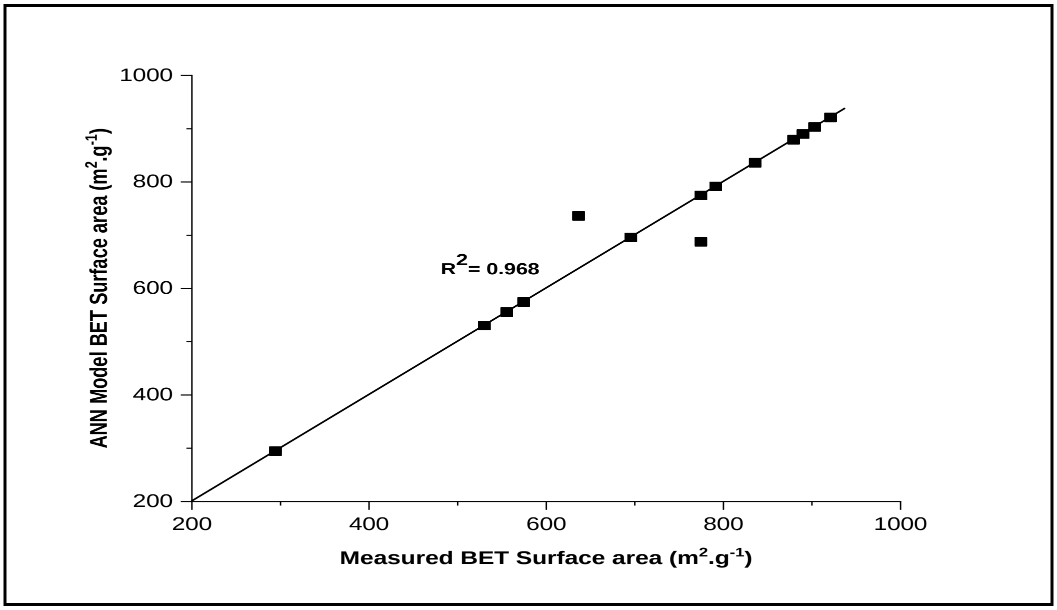

Figure 11: Cross-plot of ANN model predicted and measured results for the ZAPS activation process.

Figure 11 shows a strong correlation between the ANN predicted values and experimental results evidenced by a high coefficient of determination (R^2) value of 0.968. According to Singh et al. (2014), an R^2 value greater than 0.67 signifies excellent predictive accuracy for a non-linear regression model. Consequently, the neural network model effectively captured the activation parameter patterns, enabling precise prediction of periodic changes in the BET surface area(s) of ZAPS.

3.3. Comparative Analysis of ANN BET and RSM models

The prognostic accuracy of the response surface (RS) and artificial neural network (ANN) BET models were evaluated using performance metrics such as Root-Mean-Square-error (RMSE), correlation coefficient (R), and the squared loss function, as summarized in Table 8. Amongst these, the squared loss function provides a more insightful assessment of model performances due to its non-negative nature and high sensitivity to outliers at individual data-points (Gokcesu & Gokcesu, 2023).

Table 8: Comparison of ANN BET and RSM models for activation of ZAPS.

Run No	**RSM**	**ANN**
	Square residual	**Square residual**
1	308469.2	$1.0611E^{-20}$
2	9103.068	$3.23E^{-22}$
3	9103.068	9957.30
4	1116.228	$7.821E^{-22}$
5	22452.03	$2.551E^{-22}$
6	1.4161	$1.047E^{-24}$
7	7518.624	$6.154E^{-20}$
8	22452.03	$1.324E^{-20}$
9	9331.56	$4.864E^{-22}$
10	1011.24	7613.179
11	2962.625	$1.204E^{-19}$

12	9331.56	$1.847E^{-21}$
13	103684	$9.562E^{-22}$
14	0	$9.562E^{-22}$
15	0	$9.562E^{-22}$
16	19656.04	$1.061E^{-20}$
17	9103.068	$3.227E^{-22}$
18	9103.068	9957.30
19	1116.228	$7.822E^{-22}$
20	22452.03	$2.552E^{-22}$
21	1.4161	$1.047E^{-24}$
22	7518.624	$6.154E^{-20}$
23	22452.03	$1.324E^{-20}$
24	9331.56	$4.864E^{-22}$
25	1011.24	$5.326E^{-22}$
26	2962.625	$1.204E^{-19}$
27	9331.56	$1.847E^{-21}$
28	213628.8	$1.061E^{-20}$
29	9103.068	$3.227E^{-22}$
30	9103.068	9957.30
31	1116.228	$7.821E^{-22}$
32	22452.03	$2.551E^{-22}$
33	1.4161	$1.047E^{-24}$
34	7518.624	$6.154E^{-20}$
35	22452.03	$1.324E^{-20}$
36	9331.56	$4.864E^{-22}$
37	1011.24	7613.18
38	2962.625	$1.204E^{-19}$
39	9331.56	$1.847E^{-21}$
40	213628.8	$1.061E^{-20}$
41	9103.068	$3.23E^{-22}$
42	9103.068	9957.30
43	1116.228	$7.822E^{-22}$
44	22452.03	$2.551E^{-22}$
45	1.4161	$1.047E^{-24}$
46	7518.624	$6.154E^{-20}$
47	22452.03	$1.324E^{-20}$
48	9331.56	$4.864E^{-22}$
49	1011.24	$5.33E^{-22}$
50	2962.625	$1.204E^{-19}$
51	9331.56	$1.85E^{-21}$
52	103684	$9.562E^{-22}$
53	0	$9.562E^{-22}$
54	0	$9.562E^{-22}$
	RMSE= 157.54	**RMSE** = 31.93

The ANN BET model exhibits significantly lower squared-error residual values, ranging from 1.407×10^{-24} to 9957.30, compared to the RSM model, which has residuals ranging from 1.416 to 308469.2 (Table 8). The vast difference in the magnitude of residuals demonstrates that the ANN model provides more precise estimates of the BET surface area, thereby minimizing deviations from experimental data. The RSM model's larger residuals suggest that it provides less accurate predictions across all data points, making it less reliable than ANN.

The ANN model yields a correlation coefficient of 0.9838, significantly higher than the 0.882 obtained for the RSM model. The correlation coefficient (R) measures the strength of the relationship between predicted and experimental values. The closer R is to 1.0, the stronger the correlation. The ANN model's R-value of 0.9838 indicates an almost perfect linear relationship between experimental and predicted BET surface areas, while the RSM model's 0.882 suggests a weaker fit with higher deviations. This suggests that the ANN model has superior predictive capability and is a better fit to the experimental data. Moreover, Table 8 and Figure 12 showed the respective Root-Mean-Squared-error (RMSE) values for the RSM and ANN BET models. The RMSE, which measures the average deviation of predicted values from actual values, was significantly lower for the ANN model (31.93) than for the RSM model (157.54). The smaller RMSE value confirms the ANN model's higher accuracy and precision in generalization across various experimental conditions. In contrast, the RSM model's larger RMSE value suggests a higher degree of error in its predictions, making it less reliable for accurately modeling the $ZnCl_2$/APS system. These observations are corroborated by findings made by Nur *et al*. (2019) and Mu'azu (2022), which reported that ANN analysis performed better than RSM in computational accuracy.

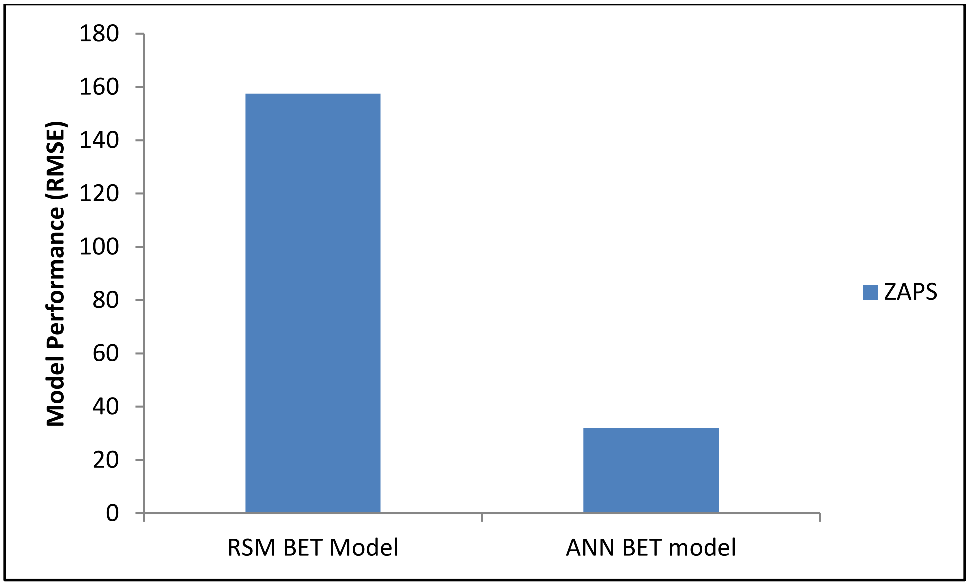

Figure 12: Model BET prediction performances for ZAPS activation process.

The superior performance of the ANN model can be attributed to multiple (embedded) hidden layer(s) and activation functions, allowing it to learn intricate patterns from data, resulting in more accurate predictions. The RSM model, which is polynomial-based, assumes a limited functional relationship between variables, making it less effective in capturing the highly non-linear interactions between activation parameters (temperature, time, and impregnation ratio) and the resulting BET surface area. As well, ANN is less sensitive to noise or outliers in the data due to its optimization algorithm(s) that adjusts the network weights to minimize prediction errors and thus, can generalize well from the labelled (training) data. In contrast, RSM models rely on pre-defined polynomial equations, that can be affected by noise and consequently, lead to suboptimal predictions (Calvacanti *et al*. 2021; Mu'azu., 2022). These findings demonstrate that the ANN model is the more effective tool for modeling the $ZnCl_2$-activated APS fabrication process, ultimately facilitating improved process understanding and optimization.

3.4. Sensitivity analysis

Sensitivity study(s) was conducted to assess the effects of the independent variables (i.e. activation time, impregnation ratio and activation temperature) on the ANN BET model output(s) and thus, elucidate the underlying rationale for predicted network result(s). The less or more the independent variable affects the ZAPS activation process, the lower or higher the corresponding sensitivity (S) value (Nkurlu *et al*., 2020). In Fig 13, activation temperature had more significant effect on the ANN predicted response (BET Surface area) than activation time and impregnation ratio with a higher sensitivity (S) value of 88.9%. This is supported by the fact that temperature rise results in pore enlargement and increment in BET surface area of activated carbon (Marsh and Rodriguez-Reinoso, 2006).

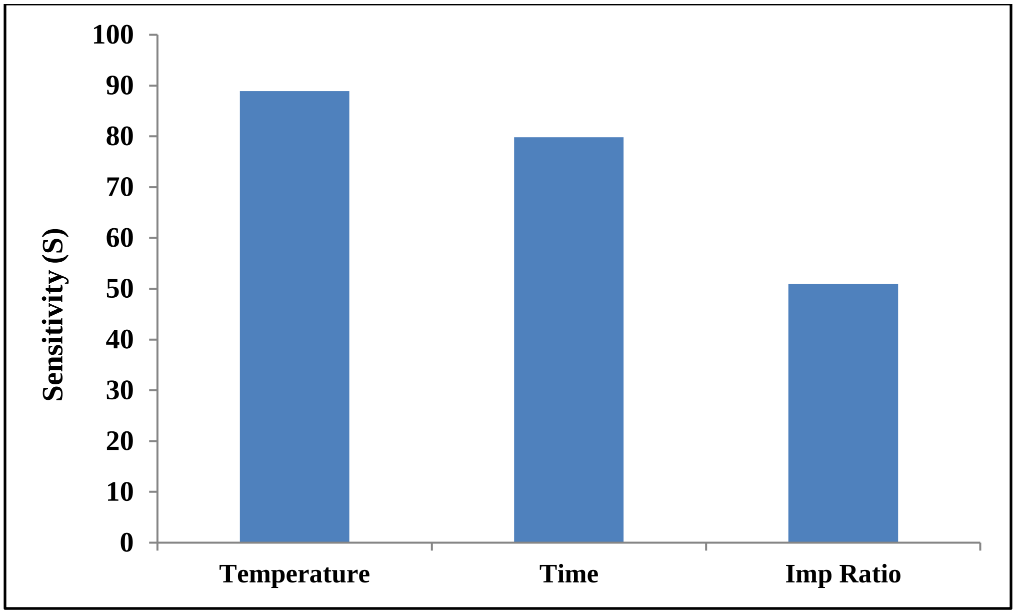

Figure 13: Impact of independent factors on ANN model predicted BET surface area for $ZnCl_2$/ZAPS system.

The lower S values of 79.84% and 50.92% ascertained for contact time and impregnation ratio respectively, signifies that both variables have reduced effect(s) on the ANN BET model prediction(s).

4.0. Conclusion

In this study, the relatively novel Artificial Neural Network (ANN) and Response Surface Methodology (RSM) assisted Box Behnken Design (BBD) tools were applied to optimize the $ZnCl_2$-activated avocado pear seed (APS) production process. The ANN and RSM models, developed using the Levenberg-Marquardt optimization algorithm and regression analysis, respectively, demonstrated high accuracy in predicting BET surface area(s). Optimization results indicated that the maximum BET surface area for $ZnCl_2$-activated APS was 457.16 m^2/g, achieved under optimal conditions: an activation temperature of 813.94°C, an impregnation ratio of 0.84, and a processing time of 67.64 minutes. The optimized ANN model incorporated three independent variables and featured two hidden layer(s), with five neurons in the first layer and four in the second. To evaluate the predictive performance of the models, Root Mean Square Error (RMSE) and the correlation coefficient (R) were used as key assessment metrics. With the highest correlation coefficient (0.9838) and minimum RMSE (31.93), the ANN predictive model was confirmed to be better compared to RSM model. Further, the sensitivity analysis results revealed that the activation temperature had the most significant impact on the ANN model prognostic performance. Concluding, the $ZnCl_2$ alkali activation of raw avocado pear seeds showed good potential for producing of quality activated carbons with high BET surface area(s).

5.0. Recommendations

The following recommendations were suggested based on this study:
The integration of Artificial Neural Networks (ANN) with optimization techniques like Genetic Algorithms (GA) or Particle Swarm Optimization (PSO) could likely enhance prediction accuracy, leading to more robust hybrid models for optimizing the $ZnCl_2$ activation process. By incorporating additional variables such as precursor type, heating rate, and cooling method, the model's accuracy and robustness could also be improved. A comparative analysis of $ZnCl_2$-activated APS performance against other commonly used activating agents, such as KOH and H_3PO_4, would also help in identifying the most effective activator for producing activated carbon from avocado pear seeds. Finally, exploring eco-friendly and renewable activating agents could contribute to the development of a more sustainable activation process.

References

Ajemba, R. O. 2012. Thermodynamics and kinetic modeling of the dissolution and adsorptive applications of Ukpor, Udi, and Nteje clays. Unpublished PhD Dissertation, Department of Chemical Engineering, Nnamdi Azikiwe University, Awka. xvi+378

Ali, R.A., Hamad, H.A., Hussien, M.H., and Malash, G.F. 2016. Potential of using green adsorbent of heavy metal removal from aqueous solutions: Adsorption kinetics, isotherm, thermodynamics, mechanism and economic analysis. *Ecological Engineering*. 91, 317-332.

Alkhasawneh, M. S. 2021. A comparison between seven heuristic methods to estimate the number of hidden layer neurons in a multi-layer perceptron neural network. *International Journal of Advanced Trends in Computer Science and Engineering*, 10(2), 1-12.

Anderson, and Whitcomb. 2016. RSM Simplified. (2^{nd} Eds). New York, USA: Productivity Inc.

Bhowmik, K.L., Debnath, A., Nath, R.K., Das, S., Chattopadhyay, K.K., and Saha, B. 2016. Synthesis and characterization of mixed phase manganese ferrite and hausmannite magnetic nanoparticle as potential adsorbent for methyl orange from aqueous media: artificial neural network modeling. *Journal of Molecular Liquids*. 219, 1010-1022.

Bodzek, M., Konieczny, K., and Kwiecinska-Mydlak, A. 2020. Nanotechnology in water and wastewater treatment. Graphene-the nanomaterial for next generation of semipermeable membranes. *Critical reviews in Environmental Science and Technology*. 50, 1515-1579.

Buasri, A., Sirikoom, P., Pattane, S., Buachum, O., and Loryuenyong, V. 2023. Process Optimization of Biodiesel from Used Cooking Oil in a Microwave Reactor: A Case of Machine Learning and Box–Behnken Design. *ChemEngineering*, 7(4), 65.

Chebii, S. J., Mukolwe, M. M., and Ong'or, B. I. 2022. River flow modelling for flood prediction using artificial neural network in ungauged Perkerra catchment, Baringo County, Kenya. *Water Practice and Technology*, 17(4), 914-929.

Du, S., Huang, Z., Jin, L., and Wan, X. 2024. Recent Progress in Data-Driven Intelligent Modeling and Optimization Algorithms for Industrial Processes. *Algorithms*, 17(12), 569.

Gokcesu, K., and Gokcesu, H. 2023. *A Note On Nonlinear Regression Under L2 Loss*. Retrieved from :https://doi.org/10.48550/ARXIV.2303.17745/., On February 13, 2024.

Goswami, L., Pakshirajan, K., and Pugazhenthi, G. 2020. Biological treatment of biomass gasification wastewater using hydrocarbonoclastic bacterium Rhodococcus opacus in an up-flow packed bed bioreactor with a novel waste-derived nano-biochar based bio-support material. *Journal of Cleaner Production*. 256, 120-253.

Haki, A. M., Imgharn, A., Aarab, N., Hsini, A., Essekri, A., Laabd, M., El Jazouli, H., Elamine, M., Lakhmiri, R., and Albourine, A. 2022. Efficient removal of crystal violet dye from aqueous solutions using sodium hydroxide-modified avocado shells: Kinetics and isotherms modeling. *Water Science and Technology*. 85(1), 433-448.

He, X., Chen, X., Wang, X., and Jiang, L. 2023. Optimization of activated carbon production from corn cob using response surface methodology. *Frontiers in Environmental Science*, *11*, 1105408.

Howard, S.P., Rowe, D. R., and Tchobanogolous, G. 1986. Environmental Engineering. Singapore: McGraw-Hill.

Ibrahim, A. A., Ibrahim, M. A., and Yusuf, A. G. 2021. Implications of industrial effluents on surface water and ground water. *World Journal of Advanced Research and Reviews*. 9(3), 330-336.

Ighalo, O.J., Yao. B, Zhou, Z.Y., and Rangabhashiyam, S. 2022. Utilization of avocado (Persea americana) adsorbents for the elimination of pollutants from water: a review. In book: Biomass-Derived Materials for Environmental Applications. Netherlands: Elsevier.

Iheanacho, C.O., Nwabanne, J.T., and Onu, C.E. 2019. Optimum process parameters for activated carbon production from rice husk for phenol adsorption. *Current Journal of Applied Science and Technology*. 36 (6), 1–11. Doi: 10.9734/cjast/2019/v36i630264.

Jafarinejad, S. 2017. Environmental Impacts of the Petroleum Industry, Protection Options, and Regulations. In Petroleum Waste Treatment and Pollution Control. Netherlands: Elsevier. 85-116.

Jerry, A.D. 2002 Neural networks. *In* M. Schwartz (Ed). *Encyclopedia of smart materials*._New York: John Wiley & Sons Inc. pp.682-689.

Kato,S., and Kansha, Y. 2024. Comprehensive review of industrial wastewater treatment techniques. *Environmental Science and Pollution Research*. 31, 51064-51097.

Li, R. Y. M., Fong, S., and Chong, K. W. S. 2017. Forecasting the REITs and stock indices: Group Method of Data Handling Neural Network approach. *Pacific Rim Property Research Journal*, 23(2), 123-160.

Machado Cavalcanti, F., Emilia Kozonoe, C., André Pacheco, K., and Maria de Brito Alves, R. 2021. Application of Artificial Neural Networks to Chemical and Process Engineering. *IntechOpen*. Doi: 10.5772/intechopen.96641

Malik, D. S., Jain, C. K., and Yadav, A. K. 2017. Removal of heavy metals from emerging cellulosic low-cost adsorbents: A review. *Applied Water Science*, 7(5), 2113–2136.

Marsh, H., and Rodríguez-Reinoso, F. 2006. Activated carbon (1st ed). Netherlands: Elsevier.

Melvin, S. S., Abigail, M. E. A., and Chidambaram, R. 2015. Isotherm modelling , kinetic study and optimization of batch Parameters using response surface methodology for effective removal of Cr (VI) using fungal biomass. *PLOS One*, 10(3), 1-13.6.

Montgomery, D.C., 2017. Design and Analysis of Experiments. New Jersey, USA: John Wiley and Sons.

Mu'azu, N. D. 2022. Insight into ANN and RSM Models' Predictive Performance for Mechanistic Aspects of Cr (VI) Uptake by Layered Double Hydroxide Nanocomposites from Water. *Water*, 14(10), 1644.

Müller, A., Österlund, H., Marsalek, J., and Viklander, M. 2020. The pollution conveyed by urban runoff: A review of sources. *Science of The Total Environment*, 709, 136125.

Nooshin, A., and Hamid, Z. 2017. Optimization of organosolv pretreatment of rice straw for enhanced biohydrogen production using Enterobacter aerogenes. *Bioresource Technology*, 227, 335-344.

Nur, S.R.T., Mohd, I.E.H., Siti, S.A.G., Uswatun, H.Z., and Mohd, Y.A.S. 2019. Artificial neural networks (ANNs) and response surface methodology (RSM) approach for modelling the optimization of chromium (vi) reduction by newly isolated acinetobacter radioresistens strain ns-mie from agricultural soil. *Hindawi Biochemistry and Medical Research International*, 1-14. Doi: 10.1155/2019/5785387.

Nguyen, T.T., Lee, S.H., and Kim, J.H. 2022. Statistical Analysis of Activation Parameters in $ZnCl_2$-Activated Carbon from Agricultural Waste. *Carbon*, 196, 123-135.

Okewale, A. O., Igbokwe, P. K., and Adesina, O. A. 2015. Optimization of the adsorptive dehydration of ethanol-water system. *Chemical and Process Engineering Research*, 39(3), 27-37.

Okiy, K., and Nwabanne, J. 2024. Optimizing Activated Carbon Production from Waste Cashew Nut Shell with Zinc Chloride: A Box-Behnken Design and Group Method of Data Handling (GMDH) Application. *Journal of the Turkish Chemical Society Section B: Chemical Engineering*, 7(1), 25-42.

Okpe, E.C., Asadu, C.O., and Onu, C.E. 2018. Statistical analysis for Orange G adsorption using kola nut shell activated carbon. *Journal of the Chinese Advanced Materials Society*. 1-15. Doi: 10.1080/22243682.2018.1534607.

Onu, C. E., Nwabanne, J.T., Ohale, P.E., and Asadu., C.O. 2021. Comparative Analysis of RSM, ANN and ANFIS and the mechanistic modeling in eirochrome black-T dye adsorption using Modified clay. *South African Journal of Chemical Engineering*. 36, 24-42.

Palani, G., Arputhalatha, A., Kannan, K., Lakkaboyana, S. K., Hanafiah, M. M., Kumar, V., and Marella, R. K. 2021. Current Trends in the Application of Nanomaterials for the Removal of Pollutants from Industrial Wastewater Treatment-A Review. *Molecules*, 26(9), 2799.

Ranade, N. V., and Ranade, V. V. 2023. ANN based surrogate model for key Physico-chemical effects of cavitation. *Ultrasonics Sonochemistry*, 94, 106327.

Singh, S.K, Jain, S.K., and Bardossy, A. 2014. Training of artificial neural network using information rich data. *Hydrology*.pp. 40-62.

Srivastava, S., Agrawal, S.B., & Mondal, M.K. 2015. A review on progress of heavy metal removal using adsorbents of microbial and plant origin. *Environmental Science and Pollution Research*. 22(20), 15386-154515.

Suzuki, M. 1990. Adsorption engineering. Kodansha ; Elsevier, Netherlands.

Van Dyk, L. D. 2000. The Production of Granular Activated Carbon from Agricultural Waste Products. Unpublished Master's Thesis, Stellenbosch University, South Africa. xi+170.

Yang, X., Wan, Y., Zheng, Y., He, F., Yu, Z., Huang, J., Wang, H., Ok, Y. S., Jiang, Y., and Gao, B. 2021. Surface functional groups of carbon-based adsorbents and their roles in the removal of heavy metals from aqueous solutions: A critical review. *Chemical Engineering Journal*, 366, 608-621.

Zhu, Y., Kolar, P., Shah, S. B., Cheng, J. J., and Lim, P. K. 2016. Avocado seed-derived activated carbon for mitigation of aqueous ammonium. *Industrial Crops and Products*, 92, 34-41.